

Coherent solutions to roll damping derivatives evaluation for a generic rocket model

Ionuț BUNESCU ^{1,2*}, Ștefan BOGOS ^{1*}, Teodor-Viorel CHELARU ^{2*}, Mihai-Vlăduț HOTHAZIE ^{1,2*}, Mihai-Victor PRICOP ^{1*}

^{1*} National Institute for Aerospace Research "Elie Carafoli"
061126 Bucharest, Romania

^{2*} University Politehnica of Bucharest: Faculty of Aerospace Engineering
060042 Bucharest, Romania

[†] Corresponding Author: bunescu.ionut@incas.ro

Abstract

A coherent approach to evaluate the roll damping derivatives for the standard Basic Finner Model is developed and presented. Results from different methods like experimental testing, numerical simulations and semi-empirical models are properly combined in order to get the best out of every method. The study aims to evaluate the reliability and accuracy of these methods and to identify the factors that contribute to their sensitivity. The paper concludes by summarizing the findings of the study and discussing the implications of the results for the design and operation of the rockets. The fusion of experimental and numerical analysis provides a robust and comprehensive evaluation of the roll damping coefficient.

1. Introduction

The prediction of the aerodynamic stability coefficients of the aerospace vehicles presents a considerable importance in the design activities. One of the most important aerodynamic stability coefficients are the damping derivatives which are very difficult to obtain due to the dynamic character. The roll damping coefficient represents the roll moment coefficient derivative with reduced rotation and it is important for lateral-directional stability and controllability of rockets, missiles or aircrafts. This coefficient can be obtained on experimental way (using flight tests or wind tunnel tests) or on numerical way (using CFD or analytical models), but both ways present several advantages and disadvantages. The experimental determination involves a large cost, the existence of an experimental infrastructure, special equipment and sensors, correction methods, compliance with some similitude criteria, large times for model manufacturing and instrumentation, limited application field, specialized operation team and others, but this kind of testing offers accurate results, short testing times once the model is available, possibility to study complex models and complex phenomena. Otherwise, the numerical prediction involves the availability of HPC resources, large times for computing, specialized operation team, reduced accuracy for complex problems and others, but this method presents smaller costs, no correction methods, no compliance with some similitude criteria and a broad field of application.

This paper continues the studies performed in the papers [1], [2], [3], [4], [5], [6], [7], [8] [9] and [10] related to roll damping coefficient determination considering both numerical and experimental methods. Although many methods for roll damping coefficient prediction already exist, this study focuses on their operational costs, applicability and accuracy. The paper presents a comparison between several coherent solutions to roll damping derivatives evaluation considering a standard dynamic model.

The methods analyzed in this paper are: the *semi-empiric method* presented in the reference [1], the *panel method* presented in references [11] and [12], which is based on potential flow model, the *Multiple Reference Frame and Sliding Mesh Technique* presented in references [4] and [5], which are based on URANS model, and the *free and forced rotation methods* presented in reference [10], which are experimental methods.

1.1. Calibration model

The model used to perform the mentioned studies is known as *Basic Finner Model* or as *Army-Navy Finner* that is a common research model for dynamic application proposed by STAI and AGARD organizations [8]. This model represents a calibration model because it is intensely used for experimental testing or numerical simulations in validation test cases. The drawing of the Basic Finner Model with is shown in Figure 1 and the isometric view of the model is shown in Figure 2.

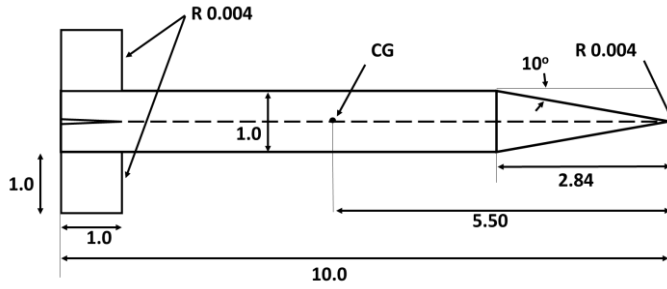


Figure 1: Basic Finner Model - technical drawing

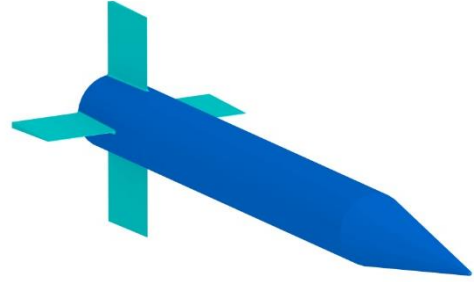


Figure 2: Basic Finner Model - isometric view

The caliber of the model used is 60mm and the model's length is 600mm according to Figure 1. The considered reference area is cross-section fuselage area (2827.43mm^2) and the model's moment of inertia around Ox axis is $I_{xx}=0.0073\text{ kg m}^2$ considering steel alloy.

1.2. Flow parameters

Each determination method presents limitation in analysis and therefore the Table 1 presents the flow parameters:

Table 1: Flow parameters

Methods	Flow parameters
Semi-empirical	Mach = 0.1 .. 3.5 at AoA = 0°
Panel Method	Mach = 0.1 .. 0.5 at AoA = $0^\circ - 20^\circ$
CFD	Mach = 0.4 .. 3.5 at AoA = 0° & Mach = 0.4, 2.5 at AoA = $0^\circ .. 50^\circ$
Experimental	Mach = 0.4 .. 3.5 at AoA = 0° & Mach = 0.4, 2.5 at AoA = $0^\circ .. 20^\circ$

2. Determination methods

Some of the first papers [13], [14] related to roll damping coefficient estimation for an aerospace vehicle, present semi-empirical methods based on experimental data for generic configurations. In the same period, experimental ballistic studies [15] were performed for roll damping coefficient determination, followed by experimental studies in wind tunnels using different techniques [6], [7], [8], [9] and [10]. Besides the experimental investigations, numerical methods were developed to predict the roll damping coefficient as an alternative to experimental testing [2], [4], [5], [16], [17], [18], [19].

Nowadays, although there are many methods for roll damping derivative evaluation, these present different levels of accuracy, limited applicability or significant resources and therefore this study focuses on their performances. The next section introduces the considered methods.

2.1. The semi-empirical method

The semi-empirical method used to determine the roll damping coefficient is based on the analytic approach of interferences and on the extrapolation of experimental data obtained for general configurations. The expression of roll damping coefficient for the considered model is:

$$C_{l_p} = 4\chi\sqrt{\vartheta_f}(K + K_F)k_1C_L^\alpha \quad (1)$$

where: χ and k_1 are coupling parameters, which creates side force and yaw moment in roll motion, ϑ_f is the air flow braking factor, K and K_F are the interference factors for wing and fuselage, and C_L^α is the lift slope with incidence.

The interference factors K includes trapezoidal correction, boundary layer correction, compressibility correction, anterior and posterior fuselage length correction and air flow breaking correction. The expression of each factor from equation (1) is presented in references [1] and [20].

2.2. The potential flow analysis

The pressure distribution on the surface S for Basic Finner configuration, from Figure 3 is evaluated by analysis of a perfect incompressible fluid flow in an external volume R .

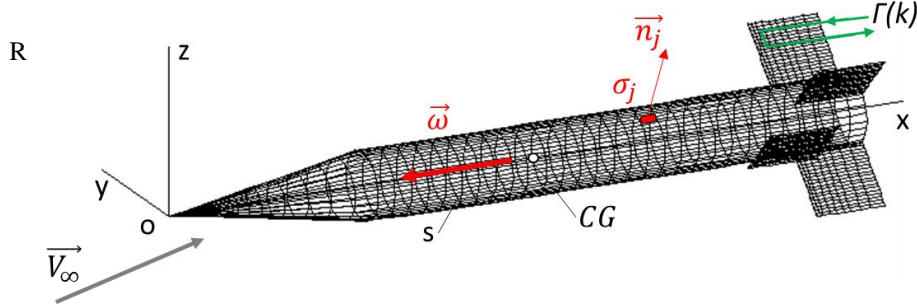


Figure 3: The formal Basic Finner aerodynamic “lattice model” with “sources” and “horseshoe vortices”

It is convenient to describe potential Φ in two components $\Phi = \Phi_\infty + \varphi$, where Φ_∞ is the potential of the freestream flow and φ is the perturbation potential due to the presence of the body. If the boundary conditions are applied to the perturbation potential φ , we obtain a Neuman Problem applied to the potential flow:

$$\begin{cases} \Delta\varphi = 0, & \text{in the region } R \\ \left(\frac{\partial\varphi}{\partial n}\right)_S = \vec{n} \cdot \vec{\nabla}\varphi = -\vec{n} \cdot \vec{V}_\infty, & \text{on the surface } S \\ \varphi = 0, & \text{at the great distances, when } r \rightarrow \infty \end{cases} \quad (2)$$

Considering an angular rotation speed $\vec{\omega}(p, q, r)$ around the center of gravity CG , the local freestream speed $\vec{V}_{\infty i}$ has the form:

$$\vec{V}_{\infty i} = \vec{V}_\infty + \vec{\omega} \times \vec{r}_i \quad (3)$$

This general approach for a general translation and rotation motion will give the damping derivatives in roll, pitch and yaw, with an important role in the dynamic analysis.

The system of equations (2) is numerically solved with particular solutions: distribution of sources $\sigma_j(q)$ on non-lifting panels and horseshoe vortices of intensity $\Gamma(k)$ on lifting zones formalized in discrete form. This robust approach is an in-house “Lattice Method” called VSLM (Vortex Sources Lattice Method) [11].

2.2. The RANS flow analysis

For the high-fidelity CFD analysis, the RANS (Reynolds Averaged Navier-Stokes) [21] model consisting of a system of partial derivative equations is used to solve the turbulent flows. The turbulence model used is the *k-ε realizable* proposed in paper [22] to solve the deficiencies of the standard model. The *k-ε realizable* model was considered because it presents good results for aerodynamic flows with roll motion as shown in papers [4] and [10].

To obtain the roll damping coefficient, two techniques were considered: the first technique is the *multiple reference frame*, which offers a quasi-steady solution, and the second technique is the *sliding mesh*, which performs an unsteady analysis rotating a small domain with the model embedded in a large domain.

The multiple reference frame approach represents a common way to model a rotating field into a fluid flow due to its simplicity and low resources required. This method transforms the components of velocity in the rotating domain considering the rolling motion in such a way that instead of the model rotating physically through the air, the air flows around the model with the corresponding velocity. The MRF approach is also known as “frozen rotor model” and its mathematical model is presented in [23]. Although the MRF approach is frequently used for industrial applications, it presents several constraints which limits its applicability:

- The rotating domain must be axisymmetric;
- The rotating axis must be concentric with the rotating parts;
- The rotating parts must be completely immersed in the rotating domain.

The sliding mesh method is the most physically correct approach for CFD analysis of rotating bodies, although this method requires large computational resources due to the unsteady character of the flow. This approach requires a distinct rotating domain and uses the interfaces to transfer information from the moving to stationary domain. In order to ensure a proper information transfer over the interface, the rotating angle per time step was imposed at 1.2° .

Both considered approaches use the same grid with a rotating domain and a stationary domain as shown in Figure 4. The first layer height of the boundary layer cells enables y^+ values around 30, in-line with the recommended size for the $k-\varepsilon$ realizable turbulence model. The final grid, presented in Figure 5, was obtained after a grid convergence study, having 9 million polyhedral cells.

The Figure 4 presents the CFD domains considered, where the diameter of stationary domain is $D = 100\text{m}$, and the rotating subdomain has a length $L = 0.75\text{m}$ and a diameter $d = 0.2\text{m}$.

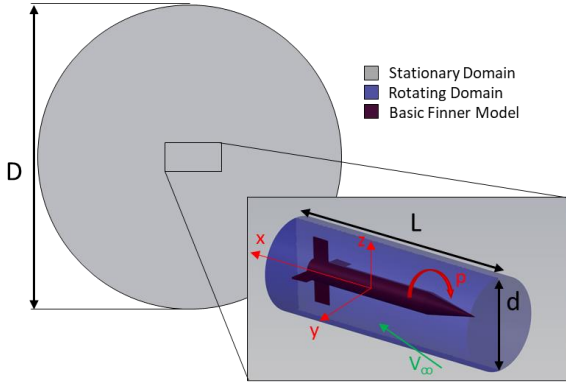


Figure 4: CFD domains

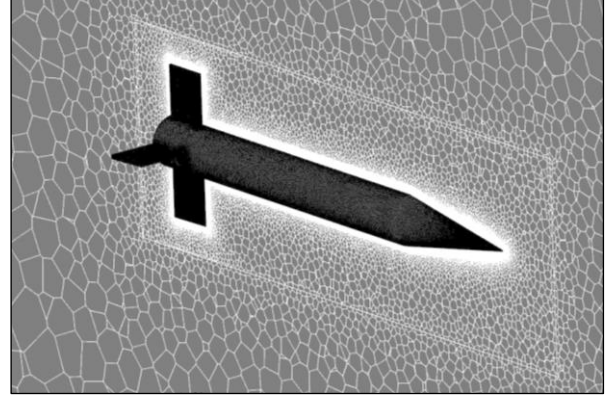


Figure 5: CFD polyhedral mesh

2.3. The experimental testing

The experimental testing in wind tunnels presents the best accuracy for aerodynamic forces and moments, but implies large operational costs and large time frames for model's manufacturing and instrumentation. The available techniques for roll damping coefficient determination through experimental testing are the forced rotation method and the free rotation method, both presenting advantages and disadvantages [24].

To obtain the aerodynamic roll damping coefficient, a special rig for dynamic test in wind tunnel was developed and used. The Roll Damping Rig (RDR) as presented in [10] allows to use both free and forced rotation methods, independently. The Basic Finner Model installed on Roll Damping Rig in the INCAS Trisonic Wind Tunnel for the experimental campaign is presented in Figure 6.



Figure 6: The BFM installed on RDR in INCAS TWT

The forced rotation method can be used by spinning the model with constant angular velocity (p_s) and measuring the roll moment (M_i) that opposes to roll motion. The division of the measured roll moment to the angular velocity gives the roll moment derivative as shown in relation (4), as in [24].

$$M_{xp} = -\frac{M_i}{p_s} \quad (4)$$

In order to obtain accurate results, the tare correction and geometry deviation correction are applied on the data sets:

$$M_{xp} = \frac{1}{2} \left[\left(\frac{M_i}{p_s} \right)^{CW} + \left(\frac{M_i}{p_s} \right)^{CCW} \right]_{WT} - \left[\frac{M_i}{p_s} \right]_{VC} \quad (5)$$

The tare correction consists in subtraction of the mechanical damping measured in vacuum chamber (VC) from the total damping measured in the wind tunnel (WT), obtaining the aerodynamic roll damping derivative. The geometry deviation correction consists in averaging the data obtained spinning the model clockwise (CW) and counter-clockwise (CCW).

The free rotation method can be used by measuring the angular velocity (p_1, p_2) of the model at distinct times (t_1, t_2), when the model is free released to rotate from an initial angular velocity such that the product between the moment of inertia and the logarithmic decay of angular velocity in time represents the roll moment derivative as in equation (6), taken from [24].

$$M_{xp} = I_{xx} \frac{\ln \frac{p_1}{p_2}}{t_2 - t_1} \quad (6)$$

The tare correction and geometry deviation procedures are performed for a higher accuracy of results using equation (7).

$$M_{xp} = I_{xx} \left\{ \frac{1}{2} \left[\left(\frac{\ln \frac{p_1}{p_2}}{t_2 - t_1} \right)^{CW} + \left(\frac{\ln \frac{p_1}{p_2}}{t_2 - t_1} \right)^{CCW} \right]_{WT} - \left[\frac{\ln \frac{p_1}{p_2}}{t_2 - t_1} \right]_{VC} \right\} \quad (7)$$

The variation of the electric current in time used by the motor to spin the model is shown in Figure 7 where the blue highlighted zone represents the time interval necessary to measure the current consumption in order to determine the roll damping coefficient using the forced rotation method. In this figure can be observed that the data acquisition for the forced rotation method last 12 seconds (four seconds for each angular speed level). The variation of the angular speed in time is presented in Figure 8 where three angular speed levels are shown, followed by a speed decay which is finally used for the free rotation method. In this case, the roll damping coefficient can be determined at any angular speed between the initial speed and the parasitic speed, although the speed damping lasts around one second for each case (the blue highlighted zone).

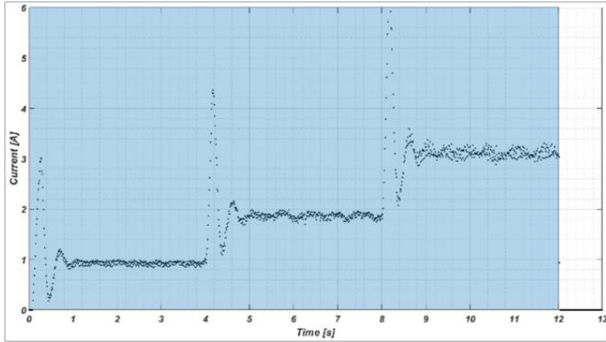


Figure 7: The variation of electric current at each angular speed

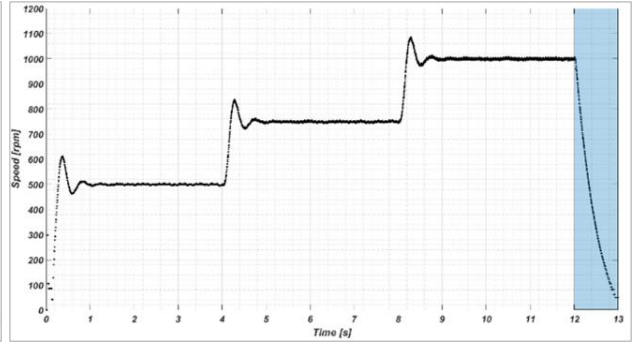


Figure 8: The variation of model's angular speed in time

3. Results and discussion

The results of the study are obtained using different methods to identify their limitations, computational resources requested and accuracy. To compare the results of the study, the variation of the roll damping coefficient with Mach number, angle of attack and angular velocity are analyzed.

3.1. Roll damping coefficient variation with Mach number

The variation of the roll damping coefficient with Mach number represents the most studied case due to its utility for aerospace vehicles which fly at small incidence over a wide Mach number range.

The Figure 9 presents the variation of C_{lp} with Mach number obtained using the semi-empirical method, the panel method, numerical methods (MRF and SMT) and experimental methods (free and forced rotation method). To compare the obtained data with a reference, a calibration data set extracted from the papers [6], [7] and [8] are considered.

The results obtained with the semi-empirical method cover the entire Mach range from 0.1 to 3.5 and the results obtained with the panel method cover just the subsonic Mach range, with a good accuracy for incompressible and low compressible flow. The CFD results obtained using MRF and Sliding Mesh techniques cover the entire Mach regime from 0.4 to 3.5. Also, the experimental results obtained using both forced and free rotation methods cover the entire Mach range.

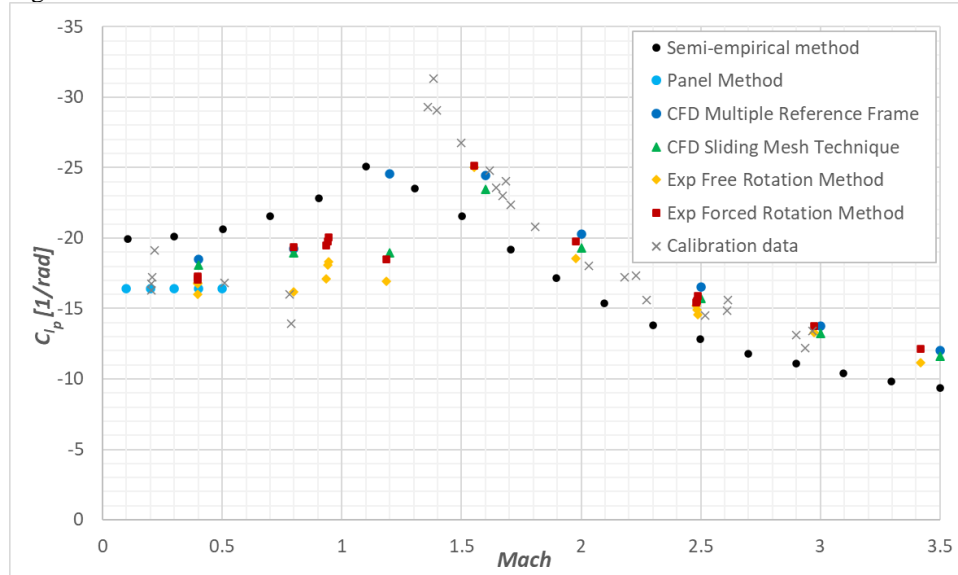


Figure 9: The roll damping coefficient variation with Mach number

Figure 9 shows that all considered methods provide results with very good accuracy related to Mach variation at 0° incidence, excepting the semi-empirical method which tends to overpredict the roll damping coefficient in subsonic and transonic regime and to underpredict in supersonic regime, but the results obtained are close to calibration data and respect the variation trend.

The values of roll damping coefficient are very well predicted in subsonic (incompressible and low compressible) and in supersonic regimes by panel method, CFD and experimental testing, but in the proximity of the transonic regime, the results of all methods are slightly dispersed.

Although the determination methods present different complexity and accuracy, the results show similar trends and present a very good accuracy, being close to the calibration data.

3.2. Roll damping coefficient variation with angle of attack

Another very important variation of roll damping coefficient is the variation with angle of attack, which is generally non-linear and difficult to predict with accuracy. The incidence of the vehicle in roll motion produces complex phenomena (flow separation and reattachment, high interferences between body and wings and shock-wave interactions).

The semi-empirical method cannot predict the variation of roll damping coefficient with the incidence, and the panel method can predict this variation with low accuracy, lacking the viscous effects. Considering the CFD method, the results depend strongly by the turbulence model, which must be able to quantify the swirling flow around a body. The MRF method cannot provide accurate data in this case because the phenomenon is strongly unsteady. Considering the experimental determination, the problem is the aerodynamic tare damping (the effect of the aerodynamic loads on the bearings) which is difficult to estimate and subtract. The only solution in this case is to spin the model with a larger velocity in order to obtain a large aerodynamic roll moment, significantly larger than the bearings friction moment.

Figure 10 presents the roll damping coefficient variation with incidence obtained using panel method, CFD with Sliding Mesh method and experimental testing with free and forced rotation methods. To analyze the roll damping coefficient variation with incidence, two relevant Mach numbers (0.4 and 2.5) were considered. A calibration data set for 2.5 Mach regime [4] is presented for results comparison.

The maximum angle of attack in experimental testing is 20°, due to limitations of the wind tunnel pitching system, while in CFD the maximum angle of attack is 50°, because the turbulence model used starts to lose accuracy at higher angles of attack.

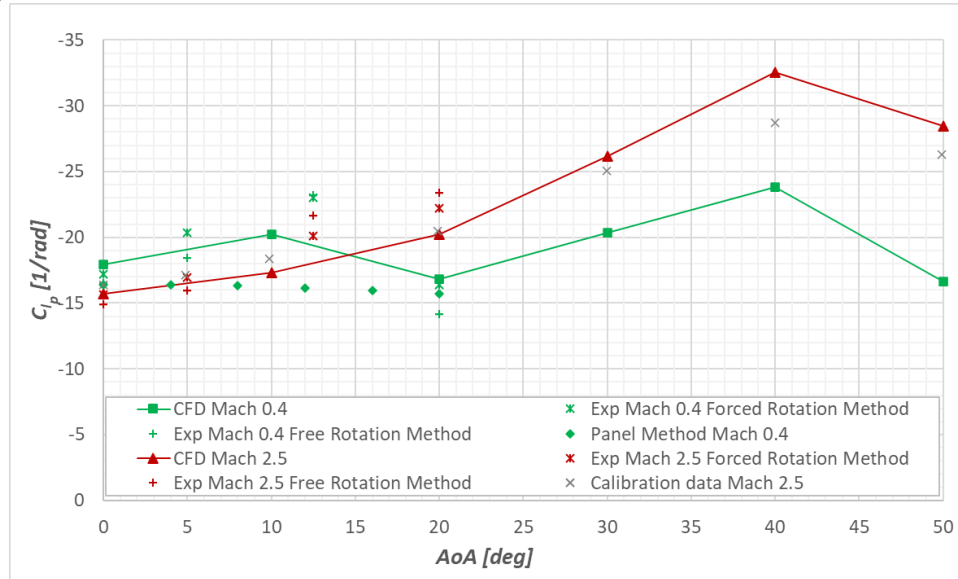


Figure 10: The roll damping coefficient variation with angle of attack

Figure 10 shows that the CFD results at Mach=2.5 fit very well the calibration data while the experimental results respect the variation trend, being close to calibration data with a small offset, that is the aerodynamic tare damping contribution. The same effect of the aerodynamic tare damping is present in subsonic regime at Mach=0.4, where the experimental data tends to overpredict the roll damping coefficient. Another remark is that for both Mach numbers, at 0° incidence, the experimental data match very well the CFD, because at this incidence the normal force on the model is zero (due symmetry) and the aerodynamic tare damping is negligible.

The results obtained with panel method present a constant variation of roll damping coefficient with incidence because the method considers the potential flow (irrotational and inviscid).

3.3. Roll moment coefficient variation with angular velocity

The variation of roll moment coefficient with angular velocity is very important for similitude criteria. If the model presents symmetry, at 0° incidence, the roll moment coefficient presents linear variation with the angular velocity, which means that the roll damping coefficient is constant with angular velocity [4], [7].

For this analysis, four representative Mach numbers (0.4, 0.95, 1.6 and 2.5) were considered and the angular velocity varies from 200 to 1000 rpm. The results were determined considering experimental testing and CFD. The semi-empirical method cannot predict the angular speed effect and the panel method cannot perform analysis at transonic and supersonic Mach regimes.

Figure 11 presents the variations of roll moment coefficient with angular velocity for the four Mach numbers. The dash-lines represents the variation trends for each Mach number, observing that the data fits the linear variation trends.

The results obtained with forced rotation method (experimental testing) and Sliding Mesh Technique (CFD) presents very accurate data with linear dependence between roll moment coefficient and angular velocity. The results obtained with MRF method tends to overpredict the values of roll moment coefficient and the results obtained with free rotation method present small deviations from the linear variation due to the sensitivity of the moment with registered angular velocity.

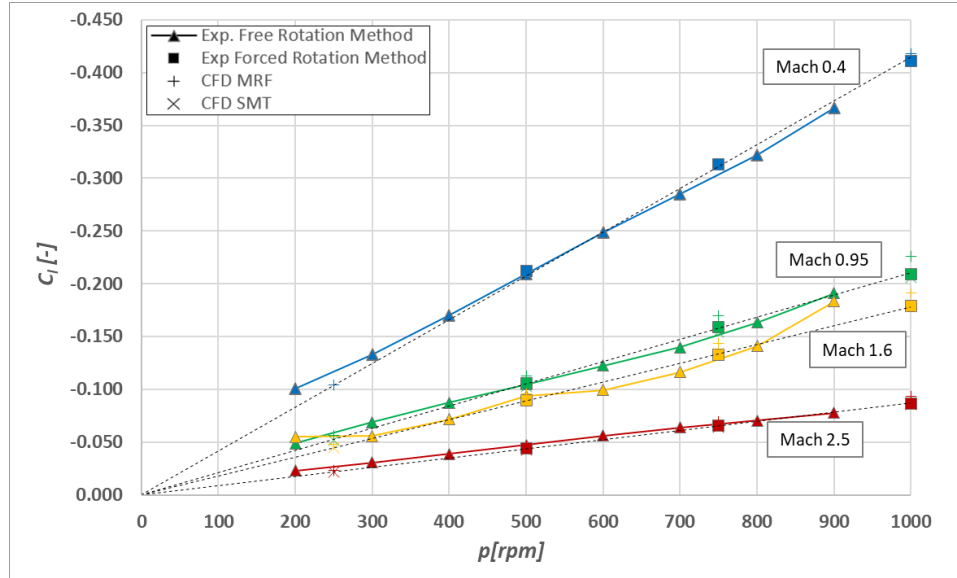


Figure 11: The roll damping coefficient variation with angular velocity

3.4. Discussion

The analyzed methods provide results with good accuracy with respect to reference data set, so that all methods are suitable for aerodynamic characterization of an aerospace vehicle but with several limits.

The semi-empirical method offers approximative values for roll damping coefficient and it is suitable only for the conceptual design of a vehicle, providing decent accuracy and capturing the Mach dependency. The limits of this method are related to geometry, incidence range and angular velocity range. The main advantage of this method is that the computational resources and computing time are very small.

The panel method provides also approximative values for roll damping coefficient and it is suitable for advanced conceptual design because it is based on a detailed geometry of the model. The results obtained with this model presents good accuracy for subsonic incompressible and low-compressible regimes. The limits of this model are related to viscous effects, incidence variation and Mach variation (for compressible subsonic, transonic and supersonic regimes). The main advantage of this method is related to small computational resources and computing time, which make it suitable for an optimization process.

The CFD methods (MRF and SMT) offer high accuracy results for roll damping coefficient and capture the effect of Mach number, angular velocity and angle of attack (only for SMT) and therefore these are suitable for preliminary design. These methods have the disadvantage of high computation resources and high computing time (3600 CPU-hours for SMT, 150 CPU-hours for MRF in this study). The main advantages of these methods are related to result's accuracy and complete characterization of flow field.

The experimental methods (forced rotation method and free rotation method) present also high accuracy results for roll damping coefficient, capturing the effect of Mach number, angle of attack and angular velocity. These methods are suitable for advanced design and analysis because the results can be obtained under full similitude criteria. The determination time are very small in this case, excepting wind tunnel model design and manufacturing. An additional inconvenient is related to wind tunnel facility which is very expensive to operate.

4. Conclusions

In conclusion, different methods for roll damping coefficient determination were presented as coherent solutions for conceptual, preliminary or advanced design of an aerospace vehicle.

Although there are simplified models for aerodynamic analysis (semi-empirical method or panel method), their results can offer useful information if are properly applied. Their main advantage is the reduced computational resources and time which makes them suitable for optimization or parametric studies.

To increase the confidence level of results or the effect of a parameter (e.g. Mach number, Reynolds number, reduced rotation, angle of attack and others) it is suitable to use more complex methods like CFD methods or experimental methods even though the requested computational/ experimental resources and time are larger.

However, the simple methods and complex methods should be used within their certainty limits and with caution according to the application. Not only the simple methods like semi-empirical and panel methods are limited,

also the CFD and experimental testing present issues. The CFD needs a pre-testing of the turbulence model, grid sensitivity analysis and convergence criteria, and the experimental methods need rigorous calibration of devices, flow control, data correction, post-processing and others.

5. References

- [1] T.-V. Chelaru, *Dinamica zborului – Îndrumar de proiect*, București: Editura Politehnic Press, 2013.
- [2] W. Gu, *Second-Order Roll Damping of Rolling Wings at Supersonic Speeds*, American Institute of Aeronautics and Astronautics, 1985.
- [3] J. Martin and N. Gerber, "The Second-Order Lifting Pressure and Damping in Roll of Sweptback Rolling Airfoils at Supersonic Speeds," *Journal of the Aeronautical Sciences*, pp. 699-704, 1953.
- [4] V. Bhagwandin, "High-Alpha Prediction of Roll Damping and Magnus Stability Coefficients for Finned Projectiles," *Journal of Spacecraft and Rockets*, vol. 53, no. 4, 2016.
- [5] H. Belaidouni, M. Samardzic, S. Zivkovic and M. Kozic, "Computational Fluid Dynamic and Experimental Data Comparison of a Missile-Model Roll Derivative," *Journal of Spacecraft and Rockets*, vol. 54, no. 3, 2017.
- [6] F. Regan, "Roll Damping Moment Measurement for The Basic Finner At Subsonic and Supersonic Speeds," NAVORD, Maryland, 1964.
- [7] B. L. Uselton and L. M. Jenke, "Experimental Missile Pitch- and Roll-Damping Characteristics at Large Angles of Attack," *Spacecraft*, vol. 14, no. 4, pp. 241-247, 1977.
- [8] H. Murthy, "Subsonic and Transonic Roll Damping Measurement on Basic Finner," *Journal of Spacecraft*, vol. 19, no. 1, pp. 86-87, 1962.
- [9] M. Samardzic, J. Isakovic, M. Milos, Z. Anastasijevic and D. B. Nauparac, "Measurement of the Direct Damping Derivative in Roll of the Two Calibration Missile Models," *FME Transactions*, vol. 41, no. 3, pp. 189-194, 2013.
- [10] I. Bunescu, M.-V. Hothazie, M.-V. Pricop and M. Stoican, "Roll Damping Measurement on Basic Finner Using Both Forced and Free Methods," in *AIAA Scitech 2023*, National Harbour, 2023.
- [11] S. Bogos, *Contributions to airplane's aerodynamics and control in take-off and landing pahses*, Bucuresti: PhD. Thesis - UPB, 2017.
- [12] J. Hess and A. Smith, "Calculation of Potential Flow About Arbitrary Bodies," *Progress in Aerospace Sciences*, vol. 8, pp. 1-138, 1967.
- [13] W. Bland and A. Dietz, "Some Effects of Fuselage Interference, Wing Interference and Sweepback on the Damping in Roll of Untapered Wings as Determined by Techniques Employing Rocket Propelled Vehicles," NACA RM L51D25, 1951.
- [14] R. McDaermon and H. Heinke, "Investigations of the Damping in Roll of Swept and Tapered Wings at Supersonic Speeds," NACA RM L53A13, 1953.
- [15] J. Nicolaides and R. Bolz, "On the Pure Rolling Motion of Winged and/or Finned Missiles in Varying Supersonic Flight," *Journal of the Aeronautical Sciences*, vol. 20, no. 3, pp. 160-168, 1953.
- [16] L. Devan, "Nonaxisymmetric body, supersonic, inviscid, dynamic derivative prediction," in *7th Applied Aerodynamics Conference*, Seattle, 1989.
- [17] S. H. Park, Y. Kim and J. H. Kwon, "Prediction of Damping Coefficients Using the Unsteady Euler Equations," *Journal of Spacecraft and Rockets*, vol. 40, no. 3, pp. 356-362, 2003.
- [18] J. Stalnaker, "Rapid Computation of Dynamic Stability Derivatives," in *42nd AIAA Aerospace Sciences Meeting and Exhibit*, Reno, 2004.
- [19] M. R. Eidell, R. P. Nance, G. Z. McGowan, J. G. Carpenter and F. G. Moore, "Computational Investigation of Roll Damping for Missile Configurations," in *30th AIAA Applied Aerodynamics Conference*, Louisiana, 2012.
- [20] M. Niță, F. Moratu and R. Patraulea, *Avioane și rachete, concepte de proiectare*, București: Editura Militară București, 1985.

- [21] O. Reynolds, "On the Dynamical Theory of Incompressible Viscous Fluids and the Determination of the Criterion," *Philosophical Transactions of the Royal Society of London*, vol. 186, pp. 123-1664, 1895.
- [22] T.-H. Shih, J. Zhu and J. L. Lumley, "A new Reynolds stress algebraic equation model," *Computer Methods in Applied Mechanics and Engineering*, vol. 125, pp. 287-302, 1995.
- [23] G. V. Shankaran and B. M. Dogruoz, "Validation of an Advanced fan model with multiple reference frame approach," in *12th IEEE Intersociety Conference on Thermal and Thermomechanical Phenomena in Electronic Systems*, 2010.
- [24] C. Schueler, L. Ward and A. Hodapp, "Techniques for Measurement of Dynamic Stability Derivatives in Ground Test Facilities," AGARD, 1967.
- [25] A. Bryson, "Stability Derivatives for a Slender Missile with Application to a Wing-Body-Vertical-Tail Configuration," *Journal of the Aeronautical Sciences*, vol. 20, no. 5, pp. 297-308, 1953.
- [26] R. Jones, "Properties of Low Aspect Ratio Pointed Wings at Speeds Below and Above the Speed of Sound," NACA , 1946.
- [27] H. Ribner, "The Stability Derivatives of Low-Aspect Ratio Triangular Wings at Subsonic and Supersonic Speeds," NACA, Washington, 1947.
- [28] J. Spreiter, "The Aerodynamic Forces on Slender Plane- and Cruciform-Wing and Body Combinations," NACA, 1950.